MAPPING CHANGES OF MIRNA-MRNA NETWORKS IN *LEISHMANIA-INFECTED* MACROPHAGES PREDICTS REGULATORY MIRNA-TF LOOPS AS NOVEL TARGETS OF PARASITE IMMUNE SUBVERSION

Charfeddine Gharsallah[1,4], Hervé Lecoeur[1], Hugo Varet[2,3], Rachel Legendre[2,3], Odile Sismeiro[3], Jean-Yves Coppée[3], Caroline Proux[3], Eric Prina[1], and Gerald F. Späth[1]

[1]Institut Pasteur, Université Paris Cité, INSERM U1201, Unité de Parasitologie Moléculaire et Signalisation, 25 Rue du Dr Roux, 75015 Paris, France; [2]Institut Pasteur, Université Paris Cité, Hub Bioinformatique et Biostatistique, 28 Rue du Dr Roux, 75015 Paris, France ; [3]Institut Pasteur, Université Paris Cité, Plate-forme Technologique Biomics, Centre de Ressources et Recherches Technologiques (C2RT), 28 Rue du Dr Roux, 75015 Paris, France. [4] Université de Tunis El Manar, Institut Pasteur de Tunis, LR11IPT02 Laboratory of Transmission, Control and Immunobiology of Infections (LTCII), Tunis, Tunisia

Abstract

MicroRNAs (miRNAs) are small non-coding RNAs that regulate gene expression at the post-transcriptional level and play a crucial role in numerous disease processes, including infections. Although intracellular microbial pathogens are known to modulate host cell gene expression to establish permissive conditions for infection, the specific role of host-encoded miRNAs underlying such subversion remains poorly understood. In this study, we employed the protozoan parasite *Leishmania amazonensis* as a model system to investigate how infection of macrophages modifies the host cell miRNA profile to evade antimicrobial functions and to establish permissive conditions for intracellular proliferation. Dual RNA-seq analyses using matched mRNA and miRNA-enriched

samples from uninfected and *L. amazonensis*-infected bone marrow-derived macrophages (BMDMs) revealed 102 differentially expressed miRNAs (padj<0.05), with 18 miRNAs showing reduced and 84 miRNAs showing increased abundance in infected BMDMs. Mapping putative networks of miRNA-mRNA interactions based on the observed expression changes, combined with Gene Ontology enrichment analyses, allowed us to identify potential miRNA target genes involved in key biological processes and metabolic pathways that permit parasite intracellular survival and proliferation. Our analyses predict the existence of a large miRNA-mRNA network affecting the expression level of numerous transcription factors that indicates inhibition of the NF-κB-dependent inflammatory response or the promotion of cholesterol biosynthesis during infection. In particular, the over 10e3-fold increase in the abundance of mmu-miR-686 in infected BMDMs was correlated with a reduced abundance of putative target transcripts implicated in miRNA biogenesis itself, in RNA binding, and in regulation of apoptosis, such as *Caspase 12*, the mRNA decay activator protein *Zfp36l1* or *Leukemia Inhibitory Factor Receptor Alpha*. Likewise, the over 200-fold increase in abundance of mmu-miR-6546-3p was associated with a reduced abundance of putative target mRNAs implicated in cytokine-mediated signaling, positive regulation of apoptotic process and regulation of gene expression, affecting, for example, the *MADS box transcription enhancer factor 2*, the *transformation related protein 53 inducible nuclear protein 1*, or the *G protein-coupled receptor 35*. Interestingly, both miRNAs are predicted to simultaneously target 32 mRNAs that showed reduced abundance in infected BMDMs, including *Maturin Neural Progenitor Differentiation Regulator* (*Mturn*), a regulator of NF-κB transcription factor activity. In conclusion, our approach provides novel insight into molecular mechanisms that may govern macrophage subversion and intracellular *Leishmania* survival. Our results shed new light on the complex relationship among miRNAs, macrophage gene expression and *Leishmania* infection, proposing regulatory feed-forward loops (FFLs) and feedback loops (FBLs) between miRNAs and TFs as a novel target of *Leishmania* immune subversion. These findings open exciting new avenues for the development of intervention strategies aimed at disrupting such crucial interactions, for example using an anti-miR (antagomir) approach against mmu-miR-686 and mmu-miR-6546-3p.

Keywords: *Leishmania*, macrophage infection, host-parasite interaction, epigenetics, microRNA, immune subversion, differential expression, network analysis.

*Correspondance: gerald.spaeth@pasteur.fr
charfeddine.gharsallah@fst.utm.tn;
herve.lecoeur@pasteur.fr;
hugo.varet@pasteur.fr;
rachel.legendre@pasteur.fr;
odile.sismeiro@pasteur.fr;
jean-yves.coppee@pasteur.fr
caroline.proux@gmail.com;
eric.prina@pasteur.fr;
gerald.spaeth@pasteur.fr.

INTRODUCTION

Epigenetic regulation is a complex mechanism that fine-tunes eukaryotic gene expression. Among epigenetic factors, microRNAs (miRNAs) have emerged as key molecules, intervening at the post-transcriptional level by targeting specific messenger RNAs (mRNAs) to modulate gene expression. Their implications extend to a wide range of human diseases, encompassing areas as diverse as cancer and microbial infections (Atri *et al.* 2019, Zhang *et al.* 2019). The importance of miRNAs lies in their ability to act as subtle regulators, actively participating in the precise adjustment of protein levels in cells. This regulation is crucial for maintaining cellular homeostasis and for the adaptive response to environmental challenges (Sprenkle *et al.* 2023). However, the influence of miRNAs is not limited to normal gene regulation. Indeed, they play a leading role in the context of microbial infections, where pathogens - whether viral, bacterial, or eukaryotic - have developed sophisticated epigenetic mechanisms to disrupt gene expression within host cells, thus ensuring their survival and replication (Ahluwalia *et al.* 2017, Sun *et al.* 2017). One of the strategies favored by these pathogens is the modulation of the expression of host miRNAs.

Leishmania are protozoan parasites that infect mammalian macrophages, inducing a significant disruption of the functions of these cells, leading to severe immune pathologies known as "leishmaniases" (McGwire and Satoskar 2014, Conceicao-Silva and Morgado 2019). The consequences of this immune subversion are varied, ranging from self-healing cutaneous forms to potentially fatal visceral forms. However, despite the magnitude of the public health problems posed by leishmaniasis and the profound impact of *Leishmania* infections on the physiology of host cells, the precise mechanisms of this immune subversion remain incompletely understood.

Recently, epigenetic subversion has emerged as a major strategy that these parasites use to escape host defenses (Kamhawi and Serafim 2020, Lecoeur *et al.* 2022, Gutierrez Sanchez *et al.* 2023). First, *Leishmania* infection has been correlated to changes in host miRNA abundance, known to limit the expression of pro-inflammatory genes, thus favoring parasite survival (Lemaire *et al.* 2013, Mukherjee *et al.* 2015, Tiwari *et al.* 2017, Muxel *et al.* 2018, Nandan *et al.* 2021, Ganguly *et al.* 2022). Second, intracellular infection by *Leishmania* causes important changes in the macrophage DNA methylation pattern, affecting signaling pathways, oxidative phosphorylation, and cell adhesion (Marr *et al.* 2014). Finally, we have previously provided the first evidence that

Leishmania also manipulates the histone code of the host cell both *in vitro* and *in vivo*, causing hypo-methylation and hypo-acetylation at promoters of pro-inflammatory genes that correlated with reduced gene expression (Lecoeur *et al.* 2020).

Here, we performed a dual RNAseq analysis to simultaneously profile changes in mRNA and miRNA abundances in primary, bone marrow-derived macrophages infected with lesion-isolated *L. amazonensis* amastigotes (Lemaire *et al.* 2013, Martinez-Hernandez *et al.* 2021, Rashidi *et al.* 2021, Fernandes *et al.* 2022, Lecoeur *et al.* 2022). Computational analysis of these data sets allowed us to map putative miRNA-mRNA regulatory networks that are predicted to control the observed inhibition of the pro-inflammatory TLR / NF-κB signalling pathway and increased cholesterol biosynthesis, both of which are prerequisites for intracellular parasite survival (Lecoeur *et al.* 2020, Gutierrez Sanchez *et al.* 2023). Our findings open new perspectives for anti-parasitic intervention targeting the non-coding transcriptome of the host cell.

MATERIAL AND METHODS

Ethics statement

Six-week-old female C57BL/6JRj and Swiss nu/nu mice were purchased from Janvier (Saint Germain-sur-l'Arbresle, France). All animals were housed in A3 animal facilities according to the guidelines of Institut Pasteur and the "Comité d'Ethique pour l'Expérimentation Animale" (CEEA) and protocols were approved by the "Ministère de l'Enseignement Supérieur, Direction Générale pour la Recherche et l'Innovation" under number 2013-0047. EP is authorized to perform experiments on vertebrate animals (license 75–1265) issued by the 'Direction Départementale de la Protection des Populations de Paris' and is responsible for all the experiments conducted personally or under his supervision as governed by the laws and regulations relating to the protection of animals.

Bone marrow-derived macrophages

Bone marrow cell suspensions were recovered from tibias and femurs of female C57Bl/6JRj mice in Dulbecco's phosphate buffered solution (PBS), and cultured in complete medium containing 4 g/L glucose, 1 mM pyruvate and 3.97 mM L-Alanyl-L-Glutamine and supplemented with 10% heat-inactivated fetal calf serum (FCS), streptomycin (50 µg/mL), and penicillin (50 IU/mL) (Sigma-Aldrich, P4333) and 50 µM β-mercaptoethanol (Sigma-Aldrich, M7522), (de La Llave *et al.* 2011). Briefly, one million cells per ml of complete medium supplemented with 50 ng/ml of mouse recombinant colony-stimulating factor 1 (rm-CSF1, ImmunoTools) were incubated in bacteriological Petri dishes (Greiner bio-one 664161) at 37°C in 7.5% CO_2 atmosphere. After 6 days of culture, the medium was removed and adherent cells were incubated with pre-warmed PBS pH 7.4 containing 25 mM EDTA for 30 min at 37°C. Bone marrow-derived macrophages (BMDMs) were detached by gentle flushing, collected, and resuspended in a complete medium supplemented with 30 ng/ml of rmCSF-1. BMDMs were seeded in 100 mm tissue culture dishes (Petri BD Falcon, 353003) for nuclear or total protein extraction and RNA isolation.

Parasite isolation and macrophage infection

mCherry-transgenic, tissue-derived amastigotes of *Leishmania amazonensis* strain LV79 (WHO reference number MPRO/BR/72/M1841) were isolated from infected footpads of Swiss nude mice (Lecoeur *et al.* 2020). After seeding at day 6 of differentiation, BMDMs were left for 5 hours at 37°C to attach to their new culture support. BMDMs were infected with lesion-derived *L. amazonensis* amastigotes at a multiplicity of infection (MOI) of 4 and then cultured at 34°C. These cells were referred to as Infected Macrophages (IMs) versus un-infected BMDMs (UIMs).

RNA extraction

Large and small (including miRNAs) RNA fractions were isolated from the same macrophage samples using the NucleoSpin miRNA kit (Macherey-Nagel) according to the manufacturer's instructions. Evaluation of RNA quality was carried out by optical density measurement using a Nanodrop device (Kisker, http://www.kisker-biotech.com). RNAs were isolated from 3 independent biological replicates of UIMs and IMs at 48 hours post-infection (PI).

RNA-Seq analysis

Library preparation and sequencing was performed at the Biomics platform of Institut Pasteur. mRNA processing: Briefly, DNAse-treated RNA extracts from Large RNA fractions were processed for library preparation using the Truseq Stranded mRNA sample preparation kit (Illumina, San Diego, California) according to the manufacturer's instructions. An initial poly A+ RNA isolation step (included in the Illumina protocol) was performed with 1 µg of large RNA to isolate the mRNA fraction and remove ribosomal RNA. The mRNA-enriched fraction was fragmented by divalent ions at high temperatures. The fragmented samples were randomly primed for reverse transcription followed by second-strand synthesis to create double-stranded cDNA fragments. No end repair step was necessary. An adenine was added to the 3'-end and specific Illumina adapters were ligated. Ligation products were submitted to PCR amplification. The quality of the obtained libraries was controlled using a Bioanalyzer DNA1000 Chips (Agilent, # 5067-1504) and quantified by spectrofluorimetric analysis (Quant-iT™ High-Sensitivity DNA Assay Kit, #Q33120, Invitrogen). Sequencing was performed on the Illumina Hiseq2500 platform to generate single-end 65 bp reads bearing strand specificity. Reads were cleaned using cutadapt

version 1.11 and only sequences at least 25 nt in length were considered for further analysis. STAR version 2.5.0a (Dobin *et al.* 2013), with default parameters, was used for alignment on the reference genome (GRCm38 from Ensembl database 94). Genes were counted using featureCounts version 1.4.6-p3 (Liao *et al.* 2014) from the Subreads package (parameters: -t gene -s 0).

miRNA processing: Sequencing was performed on the Illumina Hiseq2500 platform to generate single-end 50 bp reads with strand specificity. Reads were cleaned using cutadapt version 1.11, and only sequences with a length between 18 and 28 nucleotides were considered for further analysis. UMIs were added to read headers using umi-tools extract version 1.0.0 (Smith *et al.* 2017). Bowtie version 1.2.2 (Langmead *et al.* 2009), with default parameters, was used for alignment to the reference genome (GRCm38 from Ensembl database 92). Reads were deduplicated using umi-tools dedup to remove genuine PCR duplicates identified by UMIs. miRNAs were counted using featureCounts version v1.6.1(Liao *et al.* 2014) from the Subreads package (parameters: t miRNA -g Name -s 1) and the annotation from mirBase.

The data are publicly available at the NCBI's Gene Expression Omnibus repository (ongoing Superseries submission).

RNA-seq data analyses: Count data were analyzed using R version 3.6.1 (R-Core-Team 2016) and the Bioconductor package DESeq2 version 1.24.0 (Love *et al.* 2014). The normalization and dispersion estimation were performed with DESeq2 using the default parameters and statistical tests for differential expression were performed applying the independent filtering algorithm. A generalized linear model was set in order to test for the differential expression between the conditions For each pairwise comparison, raw p-values were adjusted for multiple testing according to the Benjamini and Hochberg (BH) procedure (Benjamini and Hochberg 1995) and genes with an adjusted p-value lower than 0.05 were considered differentially expressed.

Construction of putative miRNA/mRNA genetic interaction networks

To identify potential miRNA targets, we adopted an approach integrating computational prediction methods and experimental data, based on simultaneous profiling of miRNA and mRNA expression changes in our experimental system. Potential targets of differentially expressed miRNAs were

predicted as follows: For each differentially regulated miRNA, putative target mRNAs were first selected based on their inverse, differential expression during infection, considering an adjusted p-value of less than 0.05 as statistically significant for both miRNA and mRNA signals. We next employed the TargetScan (version 7.2) (https://www.targetscan.org/mmu_72/) (Agarwal *et al.* 2015, McGeary *et al.* 2019) and miRDB (http://www.mirdb.org/mirdb/index.html) (Chen and Wang 2020) tools associated with the miRbase database (v22) (https://mirbase.org/search/) (Griffiths-Jones *et al.* 2006, Kozomara *et al.* 2019) to screen for interactions between miRNAs and target mRNAs based on sequence complementarity. These putative associations were then visualized utilizing the Cytoscape software package (version 3.10.0) (Shannon *et al.* 2003), with each node of the predicted miRNA-mRNA networks colored based on the differential expression value (blue, decreased abundance; red, increased abundance).

Secondary structures and thermodynamic stability of prioritized miRNA sequences were predicted using the RNAfold web server (http://rna.tbi.univie.ac.at/cgi-bin/RNAWebSuite/RNAfold.cgi) (Lorenz *et al.* 2011). Additionally, we employed the RNAcomposer web server (http://rnacomposer.ibch.poznan.pl/) (Popenda *et al.* 2012) to predict the 3D structure of prioritized miRNAs. Visualization of these three-dimensional structures was performed using the BIOVIA Discovery Studio Visualizer software (https://discover.3ds.com/discovery-studio-visualizer-download). To determine the minimal free hybridization energy of these miRNAs with select potential targets, we utilized the RNAhybrid web server (https://bibiserv.cebitec.uni-bielefeld.de/rnahybrid) (Kruger and Rehmsmeier 2006).

Gene ontology and pathway analyses

Gene Ontology (GO) term enrichment analyses were conducted for all mRNAs showing differential expression between uninfected (UIM) and infected (IM) macrophages ($p < 0.05$), utilizing the GoTermFinder platform (http://www.go.princeton.edu/cgi-bin/GOTermFinder). Subsequently, the REVIGO Web server (http://www.revigo.irb.hr/) was employed to generate GO scatter plots, using the default list size (Medium: 0.7) (Supek *et al.* 2011). The associated values for each GO term represent the P-value, which is also reflected by the intensity of the bubble color. Bubble size indicates the frequency of the GO term in the underlying GO annotation (GOA)

database (bubbles of more general terms are larger). Obsolete GO terms were removed, and SimRel (default) settings was applied to measure semantic similarity.

GO terms enrichment analyses of differentially expressed miRNAs between uninfected (UI) and infected (I) macrophages ($p < 0.05$) was performed using the miEAA platform (https://ccb-compute2.cs.uni-saarland.de/mieaa/) that integrates data from different databases, such as miRBase, miRWalk et miRTarBase (Backes *et al.* 2016). miEAA is tailored for miRNA precursors and mature miRNAs from several frequently studied species, such as human, mouse, or rat. Subsequently, GO scatter plots were visualized using the REVIGO Web server as detailed above.

Gene lists used in our analyses were downloaded from the databases KEGG (Kyoto Encyclopedia of Genes and Genomes, https://www.kegg.jp/kegg/) and MGI (Mouse Genome Informatics, https://www.informatics.jax.org/), while the list of experimentally validated transcription factors was used as published by Lambert and colleagues (Lambert *et al.* 2018). The resulting gene lists were then analyzed for possible miRNAs target sites using the TargetScan platform (version 7.2) (https://www.targetscan.org/mmu_72/), which predicts potential mRNA targets of canonical miRNAs by searching for the presence of 8mer, 7mer, and 6mer sites complementary to the seed region for a given miRNA (Agarwal *et al.* 2015, Riolo *et al.* 2020). The 6mer corresponds to a perfect sequence of 6 nucleotides with the seed region of the miRNA (miRNA nucleotides 2 to 7) (Lewis *et al.* 2005). The most optimal 7mer site, referred to as 7mer-m8, features a match with the seed region strengthened by a pairing with the 8th nucleotide of the miRNA (Lewis *et al.* 2003, Brennecke *et al.* 2005, Krek *et al.* 2005, Lewis *et al.* 2005). Another 7mer site, 7mer-A1, is also effective as it includes a seed match with an 'A' at target position 1 (Lewis *et al.* 2005). Lastly, the 8mer site consists of a seed match flanked by a match at position 8 and a match with an 'A' at position 1 (Lewis *et al.* 2005). Our miRNA-mRNA interaction networks were further refined using the TargetScan parameter ‘site types’ (8mer, 7mer-m8, 7mer-1A, and non-canonical pairing) and the number of sites in all annotated 3′ UTRs. This parameter selection is based on the notion that among the presented motifs, the greater the number of nucleotides involved in pairing, the more effective the interaction will be. Thus, the type of site (e.g., whether the site is an 8mer or 7mer-m8) strongly influences repression efficacy. The number of sites also influences efficacy, with each additional site typically acting independently to confer additional repression, although sites situated between 8 and 40 nt from each other tend to act cooperatively (Grimson *et al.* 2007, Agarwal *et al.*

2015). This approach facilitates direct comparison with other studies employing TargetScan and ensures the reproducibility of our results.

RESULTS AND DISCUSSION

***L. amazonensis* subverts both the mRNA and miRNA landscapes in infected BMDMs.** Changes in miRNA and mRNA abundances were investigated in uninfected, bone marrow-derived macrophages (BMDMs, referred to as UIMs) and *L. amazonensis* infected BMDMs (referred to as IMs) established using virulent, lesion-derived amastigotes (Figure 1). Large (mRNAs) and small (primarily miRNAs) RNA fractions were isolated from these samples at day 2 post-infection (PI) and subjected to RNAseq analysis (Figure 1A). As judged by the expression changes observed across three independent biological replicates, *Leishmania* infection has a major impact on both the mRNA and miRNA profiles of IMs, with significant changes observed for the abundance of 5742 mRNAs (10.36 % of total, padj <0.05) and 102 miRNAs (6.04 % of total, padj <0.05) (Figure 1B1 and 1C1). Inspection of biological functions enriched in the differentially expressed genes (Figure 1B2) and miRNAs (Figure 1C2), revealed a series of GO terms that were previously associated with *Leishmania*-mediated immune subversion and infected macrophages and that converged in both the miRNA and mRNA datasets, including GO terms linked to inflammatory response, NF-κB signaling, apoptosis, or essential metabolic processes related to cholesterol and fatty acid biosynthesis (Figures 1B2 and C2).

Closer inspection of miRNA read depth variations during infection identified 84 miRNAs (82.4%) with and 18 miRNAs (17.6%) with decreased abundance, suggesting that intracellular *L. am* has a profound effect on the miRNA landscape in agreement with a previously published report using *L. amazonensis* infected BMDMs from BALB/c (Muxel *et al.* 2017) (figures D1 and D2 respectively). Important read depth variations were observed for mmu-miR-686 that showed an over 1000-fold increase in abundance (3 normalized reads in UIMs vs 3953 in IMs), as well as for mmu-miR-6546-3p (2 vs 891, 445-fold increase) and mmu-miR-718 (261vs 1,023, 3.9-fold increase) (figure D1). Significant increase in expression was further observed for a series of murine miRNAs with high homology to human (https://rnacentral.org/), such as mmu-miR-150-3p, mmu-miR-488-3p, and mmu-miR-299a-5p. In contrast, the strongest reduction in read depth during

infection was observed for mmu-miR-342-3p (55,522 vs 31,602), mmu-let-7b-5p (11,428 vs 7,176), mmu-miR-99b-5p (4,508 vs 1,926), mmu-miR-92a-3p (2,278 vs 611), mmu-miR-339-5p (1,271 vs 469), and mmu-miR-532-3p (741 vs 394). Decreased abundance of mmu-let-7b-5p has been also observed during infection with *L. infantum* and *L. major* in human macrophages (Geraci *et al.* 2015, Ramos-Sanchez *et al.* 2022), suggesting a key role of this miRNA in intracellular parasite infection.

In conclusion, our data confirm the differential expression of miRNAs during intracellular *Leishmania* infection, which correlated with important expression changes at mRNA levels, suggesting the existence of regulatory miRNA-mRNA networks that may govern the establishment of an immune-compromised host cell phenotype. We next applied a series of computational tools to further assess possible miRNA-mRNA regulatory interactions.

Modelling interaction networks related to reduced miRNA expression. miRNA-mRNA regulatory networks are characterized by reciprocal expression changes between both types of RNA, where increased miRNA usually causes decreased expression of its target mRNA (and *vice versa*). We investigated the existence of such networks by first focusing on down-regulated miRNAs whose expression changes are supported by at least 50 normalized reads, and their predicted mRNA targets that show increased abundance during infection (Log2 Fold Change (FC) ≥ 1, $p < 0.05$). Only 2 out of the 18 downregulated miRNAs did not pass this filtering step and were excluded (i.e. mmu-702-3p, mmu-miR-99b-5p). Down-regulation of the remaining 16 miRNAs were tightly associated with increased abundance of their predicted target mRNAs as illustrated by the interaction network shown in Figure 2A. Important differences were observed between these networks both with respect to the level of miRNA down-regulation as well as the number of possible target mRNAs (Figure 2A). For example, mmu-miR-532-3p and mmu-miR-342-3p respectively are predicted to target only 5 and 10 transcripts, while on the other extreme, mmu-484 and mmu-767 respectively are predicted to target 136 and 97 transcripts (Figure 2A). Some sets of upregulated transcripts are predicted to be solely under the control of a single miRNA, as illustrated by mmu-767 (74 transcripts), mmu-484 (36 transcripts), mmu-miR-3968 (22 transcripts), and mmu-let-7b-5p (8 transcripts). Thus, affecting a single miRNA during intracellular

Leishmania infection can generate a pleiotropic outcome with important consequences on cellular processes and diverse pathologies (Valinezhad Orang *et al.* 2014).

We next focused on the two miRNAs mmu-let-7b-5p (11,428 in UIMs vs 7,176 normalized read counts in IMs, Log2FC = -0.752) and mmu-miR-342-3p, based on (i) their significant differential read count between UIMs and IMs, (ii) their conservation to human miRNAs (Pasquinelli *et al.* 2000), https://rnacentral.org/sequence-search/?jobid=c25cc34b-01cf-42ae-a24e-611a1132aa1e), and their involvement in key biological processes, including apoptosis, Jak/Stat signaling, or NF-κB signaling (Tai *et al.* 2015, Thammaiah and Jayaram 2016, Cui *et al.* 2019, Lecoeur *et al.* 2022, Taghehchian *et al.* 2023). Consolidating our target mRNA predictions from TargetScan and miRDB platforms established a list of 192 putative mmu-let-7b-5p mRNA targets showing increased abundance during infection, including *Integrin Beta 3 subunit* (*Itgb3*, Log2 FC = 2.35), *Argonaute RISC Catalytic Component 2* (*Ago2*, Log2 FC = 1.37), *Dual-specificity phosphatase 9* (*Dusp9*, Log2 FC = 1.94) (Figure 2A) and 7 mRNAs encoding for transcription factors (TFs) or epigenetic regulators (ERs), *i.e.* *Arid3a*, *E2f6*, *Hmga1*, *Klf8*, *Nr6a1*, *Pbx1*, and *Zfp202* (Figure 2B), which are involved in regulation of proliferation regulation, cell differentiation, DNA structure modification, and cancer-related signaling pathways (Trimarchi *et al.* 2001, Patterson *et al.* 2008, Wang *et al.* 2022, Guo *et al.* 2023, Bai *et al.* 2024, Kao *et al.* 2024, Zhang *et al.* 2024).

Likewise, decreased expression of mmu-miR-342-3p was associated with increased expression during infection of 75 putative mRNA targets, including *Syndecan 1* (*Sdc*1, Log2 FC = 2.37), *LDL Receptor Protein 8* (*Lrp*8, Log2 FC = 2.82) (Figure 2A) and 9 TFs/ERs (*Cebpg*, *Gmeb1*, *Jazf1*, *Kmt2a*, *Pou3f1*, *Sox7*, *Tcf12*, *Zbtb21*, and *Zbtb42*) (Figure 2B), which regulate genes involved in several biological processes such as glucocorticoid synthesis, regulated cell death or proteasomal protein degradation (An *et al.* 2019)

Both mmu-let-7b-5p and mmu-miR-342-3p share 12 predicted targets, including *Zinc Finger Protein 42* (*Zfp42*) (Log2 FC= 2.537), which shows high base pairing probability that suggests strong binding of both miRNAs (Figure 2C1). Specific interaction between both miRNAs and *Zfp42* mRNA is further supported by the low hybridization energy below -20 kcal/mol and the presence of strong 7mer-m8 and 7mer1A binding properties (Figure 2C2).

In conclusion, our analyses reveal the presence of putative miRNA-mRNA networks that may participate in increased gene expression observed during *Leishmania* infection. The identification of *Ago2* as a putative miRNA target further suggests the existence of a regulatory feedback loop during *Leishmania* infection, where miRNAs can affect their own production as seen recently in mammalian development (Liu *et al.* 2021). Furthermore, the identification of TFs as putative miRNA targets opens the possibility to control macrophage gene expression in a cooperative fashion through feed-forward loops (FFLs) and feedback loops (FBLs) (Shalgi *et al.* 2007, Tsang *et al.* 2007).

Modelling of interaction networks related to increased miRNA expression. We next applied the same filtering procedure as indicated above to establish networks between the 84 miRNA showing increased expression during infection and the 199 down-regulated mRNAs (Log2 FC ≤ -0.5). The 33 miRNAs of the network shown in Figure 3A passed this filtering step and were prioritized for network analysis considering the level of their increased expression and their high conservation with human miRNA for some of them. As expected, increased expression of these miRNAs correlated with decreased abundance of their predicted mRNA targets (Figure 3A). Important differences were observed for the number of putative mRNA targets that are predicted to interact with these miRNAs (Figure 3A), with for example mmu-miR-299a-5p predicted to target only *Ring Finger Protein 150* (*Rnf150*), or mmu-miR-6546-3p to target just 9 transcripts (including 1 TF), while mmu-miR-7661-5p is predicted to target 93 transcripts (including 6 TFs) (Figure 3A).

For subsequent analyses, we focused our attention on two highly expressed miRNAs. First, mmu-miR-686 shows an over 1000-fold increase of abundance during infection and is predicted to target 433 mRNAs that showed statistically significant reduced abundance during infection ($p < 0,05$). Putative mRNA targets showing reduced abundance in our analysis include the mRNA decay-activating protein *Zinc Finger Protein 36*, C3H Type (*Zfp36l1*, Log2 FC = -3.12), *Ribonuclease A Family Member K6* (*Rnase6*, Log2 FC = -2.4) or *Caspase 12* (*Casp12*, Log2 FC = -3.34) (Figure 3B) linking this miRNA to key biological processes such as apoptosis, cell proliferation and chromatin binding. MiR-686 has also the potential to negatively regulate the transcripts of 31 transcription factors, including *Elf4*, *Bcl6*, *Stat1*, *Foxo3*, *Hmbox1*, and *Bcl6*

(Figure 3B), adding cell proliferation, differentiation, apoptosis and antimicrobial resistance to its putative list of target processes (Spath *et al.* 2009, Lecoeur *et al.* 2022, Xu *et al.* 2024).

Second, mmu-miR-6546-3p shows an over 200-fold increase of abundance during infection and is predicted to target 117 mRNAs that showed statistically significant reduced abundance during infection ($p < 0.05$) (Figure 3B), including *G-protein-coupled receptor 35* (*Gpr35*, Log2 FC = -2.54), which facilitates the activity of the C-X-C chemokine receptor (Boleij *et al.* 2021) or the developmental TFs *MADS box transcription enhancement factor 2* (*Mef2c*, Log2 FC = -2.48) and *transformation-related protein 53-induced nuclear protein 1*, (*Trp53inp1*, Log2 FC = -1.92) (Figure 3B). mmu-miR-6546-3p has further the potential to reduce the expression of 14 transcription factors, including *Ets1*, *Foxo3* (implicated in cell death regulation, (Litvak-Greenfeld and Benhar 2012), *Mef2c*, *Rela*, *Stat2*, and *Stat3* (Figure 3B), some of which were previously linked to *Leishmania* infection, such as *Stat3* (Mishra *et al.* 2023) or *Rela*, whose mRNA abundance was reduced during *in vitro* and *in vivo L. amazonensis* infection, dampening the TLR / NF-κB / NLRP3 pathway (Lecoeur *et al.* 2020).

Both miRNAs have the potential to synergize for the negative regulation of 34 common mRNA targets, including the TFs *Maturin, Neural Progenitor Differentiation Regulator Homolog* (*Mturn*, Log2 FC = -1.559) (Figure 3B). These putative interactions are further supported by (i) strong miRNA-mRNA base pairing probability and an elevated overall thermodynamic free energy of -5.41 (mmu-miR-686) and -1.97 kcal/mol (mmu-miR-6546-3p) (Figure 3C1). In general, miRNAs with high thermodynamic stability are considered crucial for efficient transcriptional regulation, which explains their high intracellular concentrations (>1,000 molecules per cell) according to recent studies (Luna *et al.* 2015, Denzler *et al.* 2016). Furthermore, as exemplified by the putative *Foxo3* mRNA target, both miRNAs show a low hybridization energy below -18 kcal/mol and the presence of strong 8mer and 7mer1A binding properties (Figure 3C2).

In conclusion, just as observed for the miRNA^{down}/mRNA^{up} regulatory networks, the miRNA^{up}/mRNA^{down} regulatory networks described here propose miRNAs as important pleiotropic regulators that may be engaged by *Leishmania* to efficiently reprogram the host cell expression profile in favor of intracellular parasite survival.

***In silico* assessment of miRNA-mediated subversion of the TF landscape.** One striking signal emerging from our network analyses is the number of differentially expressed TFs and epigenetic regulators (ERs) that are predicted targets of miRNAs. A focused *in silico* analysis of these interactions is shown in Figure 4 that visualizes simplified networks between 15 down-regulated miRNAs and 79 upregulated TF/ER mRNAs (Figure 4, panel A), and *vice versa* between 34 upregulated miRNAs and 160 downregulated, putative TF/ER targets (Figure 4, panel B). These interactions may represent a very cost-efficient parasite immune subversion strategy, where changes in a small set of miRNAs have important consequences on macrophage expression profile and phenotype, either by directly affecting TFs/ERs or by exploiting regulatory feed-forward and feedback loops between miRNAs and TFs/ERs that could jointly control the transcriptomic reprogramming we previously described in *L. amazonensis* infected macrophages and dendritic cells (Lecoeur *et al.* 2020, Lecoeur *et al.* 2020, Lecoeur *et al.* 2022).

***In silico* assessment of miRNA-mediated suppression of the pro-inflammatory response.** We have previously identified the TLR / NF-κB axis as a prime target for epigenetic subversion of the macrophage inflammatory response by *L. amazonensis* infection that correlated with histone H3 hypo-acetylation and hypo-methylation (Lecoeur *et al.* 2020). Our data here uncover that modulation of the host miRNA landscape may constitute an additional epigenetic layer subverting pro-inflammatory signaling during infection. The focused network shown in Figure 5 identifies 16 down-regulated miRNAs that are predicted to target 16 up-regulated members of this pathway (panel A), while 28 up-regulated miRNAs are predicted to affect 24 down-regulated pathway members (panel B). Even though this one-on-one regulation may indicate only limited influence of miRNA on expression of these targets, placing these interactions into the context of the entire pathway reveals that miRNAs could affect every step of TLR / NF-κB pathway establishing the anti-inflammatory phenotype characteristic of *Leishmania*-infected macrophages (Figure 5C). miRNA^{up}/mRNA^{down} interactions are observed for a number of activating pathway members, from surface receptors that trigger the initial activation (e.g. miR-138-2-3p for *Cd40*, miR-7088-5p for *Tnfrsf1a*), down to NF-κB family members (miR-6546-3p for *Rela*, miR-546 for *Relb*, miR-299a-5p for *NFkb1*, miR-327 for *Nfkb2*) that induce inflammatory gene expression. On the contrary, miRNA^{down}/mRNA^{up} interactions are observed for deactivating pathway members, such as *Tnfaip3*

precited to be targeted by miR-92a-3p. These data reveal miRNAs as potential regulators of the dual inhibition of the macrophage pro-inflammatory response we have described previously (Lecoeur *et al.* 2020).

***In silico* assessment of miRNA-mediated induction of cholesterol biosynthesis.** Cholesterol biosynthesis represents one of the key biological processes induced during *L. amazonensis* infection believed to be essential for parasite development and vacuole membrane biogenesis (Osorio y Fortea *et al.* , Gutierrez Sanchez *et al.* 2023). Our data suggest miRNAs as possible key regulators of this pathway during *Leishmania* infection. The focused network shown in Figure 6 identifies 8 down-regulated miRNAs that are predicted to target 32 up-regulated members of this pathway (panel A), while 20 up-regulated miRNAs are predicted to affect 20 down-regulated pathway members (panel B). Placing these putative interactions in the context of the cholesterol pathway (panel C) sheds a more integrative light on the outcome of these transcriptional modulations and again proposes a dual regulation underlying increased cholesterol production. Certain miRNAs act as possible positive regulators of this pathway, with for example down-regulation of miR-532-3p correlating with upregulation of its mRNA target Sterol Regulatory Element Binding Transcription Factor 2 (*Srebf2*), a master regulator of cholesterol biosynthesis (Amemiya-Kudo *et al.* 2002). In contrast, miRNA^{up}/mRNA^{down} interactions seem to be linked to cholesterol homeostasis, as indicated by down-regulation of the ATP binding cassette subfamily A member *Abca1* (putative target for mmu-miR7661-5p) that functions as a cholesterol efflux pump (Quazi and Molday 2013), or the cytochrome P450 superfamily member CYP27A1 (putative target for mmu-miR664-3p) controlling cholesterol removal (Pikuleva *et al.* 1998).Thus the combined effect of these miRNAs likely enhances activating components of cholesterol biosynthesis while at the same time limiting cholesterol removal.

CONCLUSION

Applying dual RNAseq analysis on mRNA and miRNA fractions obtained from *L. amazonensis*-infected and uninfected BMDMs allowed us unprecedented insight into the possible role of the host cell noncoding RNome as a novel target for parasite immune subversion. Based on our

computational analyses, the observed miRNA expression changes are predicted to affect the abundance of a large array of transcripts that establish the immune-metabolomic expression profile and cellular phenotype characteristic of *L. amazonensis* infected macrophages (Zhang *et al.* 2022). The challenge for future studies lies on experimentally validating these interactions for example using RNA pull down experiments to establish defined miRNA-mRNA target relationships or applying genetic ablation on key miRNAs to study their effect on host cell gene expression and intracellular parasite survival. These future investigations will hold great promise to define miRNAs as novel, host-directed therapeutic targets against *Leishmania* using agomir and antagomir strategies to restore the anti-microbial potential of host macrophages (Rupaimoole and Slack 2017, Murdaca *et al.* 2019, Chong *et al.* 2021).

FIGURE LEGENDS

FIGURE 1: Dual RNAseq analysis of mRNA and miRNA fractions in *L. amazonensis*-infected versus non-infected macrophages. (A) Experimental pipeline for the generation of BMDMs, their infection, and isolation of large versus small RNAs. BMDMs were derived from mCSF-treated C57BL/6 bone marrow progenitors and were infected (IMs) or not (UIMs) with lesion-derived amastigotes of *L. amazonensis* for 2 days. Large and small RNAs were isolated from the same samples (n=3 independent experiments) and subjected to RNAseq analysis. **(B, C)** Heat maps, volcano plots and REVIGO enrichment maps showing respectively differentially expressed mRNAs and miRNAs across three biological replicates (1-3) in uninfected (UIMs) and infected (IMs) macrophages (B1 and B2, left panels, log2 fold changes (FC) are shown), the distribution of differentially expressed mRNAs and miRNAs according to their average, normalized read counts (B1 and C1, right panels, statistically significant signals with $p < 0.05$ are indicated in red), and biological functions enriched in the datasets of differentially expressed mRNA (B2) and miRNA (C2). Bubble color reflects the p-value of the enrichment and bubble size indicates the frequency of the GO term in the underlying GOA database. For space reasons, only few bubbles are labeled with their corresponding GO term, while others are numbered as follows: 1, Inflammatory response (GO:0006954); 2, Apoptosis process (GO:0006915); 3, Cholesterol homeostasis (GO:0042632); 4, Fatty acid biosynthetic process (GO: 0006633); 5, Fatty acid oxidation (GO: 0019395); 6, I-κB kinase/ NF- κB signaling (GO:0007249); 7, Negative regulation of NF- κB TF activity (GO:0032088); 8, Positive regulation of I-κB kinase/ NF-κB signaling (GO:0043123); 9, Response to LPS (GO: 00032496); 10, Response to protozoan (GO:0001562); 11, Macrophage activation (GO: 0042116); 12, Cytokine production involved in immune response (GO:0002367); 13, JNK cascade (GO:0007254); 14, MAPK cascade (GO:0000165); 15, Regulation of gene expression (GO: 0010468); 16, Regulation of DNA-binding TF activity (GO:0051090); 17, Positive regulation of DNA binding (GO:0043388); 19, Chromatin remodelling (GO:0006338); 20, Histone H4 acetylation (GO:0043967); 21, Epigenetic regulation of gene expression (GO:0040029); 22, mRNA transport (GO:0051028); 23, RNA-mediated gene silencing (GO:0031047); 24, Positive regulation of miRNA-mediated gene silencing (GO:0043388); 25, miRNA-mediated gene silencing by inhibition of translation (GO:0035278). **(D)** Circular heatmaps of miRNAs showing increased (D1) or decreased (D2) normalized read counts during infection. Highlighted in red and

green are miRNAs with high similarity to human miRNAs (except miR-686 and miR6546-3p). Nnr, Normalized read counts.

FIGURE 2: Gene regulatory networks between down-regulated miRNAs and putative target mRNAs showing increased abundance in infected macrophages. **(A)** Predicted interactions are shown between miRNAs (rectangles, fill color indicates level of decreased abundance in log2 FC) and mRNAs (circles, fill color indicates level of increased abundance in log2 FC). Transcription factors are indicated by the oval shape. Shown interactions are based on miRNAs showing a difference of 50 or more normalized reads between infected (IMs) and uninfected (UIMs) groups, and mRNAs showing IMs vs UIMs expression changes of Log2 FC ≥ 1. **(B)** Predicted interaction maps between down-regulated mmu-let-7b-5p and mmu-miR-342-3p and their potential target mRNAs showing increased abundance in IMs vs UIMs. **(C)** 2D and 3D structures of mmu-let-7b-5p and mmu-miR-342-3p (C1). The probability of miRNA binding to the putative target mRNA *Zfp462* is indicated by the color. Target position, length, site type and minimum hybridization energy (mfe) are indicated in panel C2.

FIGURE 3: Gene regulatory networks between up-regulated miRNAs and putative target mRNAs showing reduced abundance in infected macrophages. **(A)** Predicted interactions are shown between miRNAs (rectangles, fill color indicates level of increased abundance in log2 FC) and mRNAs (circles, fill color indicates level of decreased abundance in log2 FC). Transcription factors are indicated by the oval shape. Shown interactions are based on miRNAs showing a difference of 50 or more normalized reads between infected (IM) and uninfected (UIMs) groups, and mRNAs showing IMs vs UIMs expression changes of Log2 FC ≤ -1. **(B)** Predicted interaction maps between up-regulated mmu-686 and mmu-miR-6546-3p and their potential target mRNAs showing decreased abundance in IMs vs UIMs. **(C)** 2D and 3D structures of mmu-686 and mmu-miR-6546-3p (C1). The probability of miRNA binding to the putative target mRNA *Foxo3* is indicated by the color. Target position, length, site type and minimum hybridization energy (mfe) are indicated in panel C2.

FIGURE 4: miRNA network analyses focused on putative mRNA targets implicated in expression regulation. mRNAs encoding for transcription factors (TFs) and epigenetic regulators (ERs) showing significantly increased and decreased abundances (padj < 0.05) are shown in red (panel A) and blue (panel B), respectively. The solid lines (8mer) represent the most efficient interaction. Next are the dashed lines (7mer-m8) and dotted lines (7mer-1A), followed by the sine wave lines (non-canonical), indicating varying levels of interaction efficiency.

FIGURE 5: miRNA network analyses focused on putative mRNA targets implicated in the NF-κB pathway. mRNAs encoding for NF-kB pathway members showing significantly increased and decrease (padj < 0.05) mRNA abundances are shown in red (panel A) and blue (panel B), respectively. The solid lines (8mer) represent the most efficient interaction. Next are the dashed lines (7mer-m8) and dotted lines (7mer-1A), indicating varying levels of interaction efficiency. (C) Projection of miRNA and mRNA expression values and putative regulatory interactions on the NF-κB pathway.

FIGURE 6: miRNA network analyses focused on putative mRNA targets implicated in cholesterol biosynthesis and homeostasis. mRNAs encoding for proteins implicated in cholesterol production showing significantly increased and decrease (padj < 0.05) mRNA abundances are shown in red (panel A) and blue (panel B), respectively. The solid lines (8mer) represent the most efficient interaction. Next are the dashed lines (7mer-m8) and dotted lines (7mer-1A), indicating varying levels of interaction efficiency. (C) Projection of miRNA and mRNA expression values and putative regulatory interactions on the cholesterol biosynthetic pathway.

References

*Agarwal, V., G. W. Bell, J. W. Nam and D. P. Bartel (2015). "Predicting effective microRNA target sites in mammalian mRNAs." Elife **4**.

*Ahluwalia, P. K., R. K. Pandey, P. K. Sehajpal and V. K. Prajapati (2017). "Perturbed microRNA Expression by Mycobacterium tuberculosis Promotes Macrophage Polarization Leading to Pro-survival Foam Cell." Front Immunol **8**: 107.

*Amemiya-Kudo, M., H. Shimano, A. H. Hasty, N. Yahagi, T. Yoshikawa, T. Matsuzaka, H. Okazaki, Y. Tamura, Y. Iizuka, K. Ohashi, J. Osuga, K. Harada, T. Gotoda, R. Sato, S. Kimura, S. Ishibashi and N. Yamada (2002). "Transcriptional activities of nuclear SREBP-1a, -1c, and -2 to different target promoters of lipogenic and cholesterogenic genes." J Lipid Res **43**(8): 1220-1235.

*An, W., S. Yao, X. Sun, Z. Hou, Y. Lin, L. Su and X. Liu (2019). "Glucocorticoid modulatory element-binding protein 1 (GMEB1) interacts with the de-ubiquitinase USP40 to stabilize CFLAR(L) and inhibit apoptosis in human non-small cell lung cancer cells." J Exp Clin Cancer Res **38**(1): 181.

*Atri, C., F. Z. Guerfali and D. Laouini (2019). MicroRNAs in diagnosis and therapeutics.

*Backes, C., Q. T. Khaleeq, E. Meese and A. Keller (2016). "miEAA: microRNA enrichment analysis and annotation." Nucleic Acids Res **44**(W1): W110-116.

*Bai, Q., W. Jin, F. Chen, J. Zhu, L. Cao, Y. Yang, F. Zhong and L. Li (2024). "KLF8 Promotes the Survival of Lung Adenocarcinoma During Nutrient Deprivation by Regulating the Pentose Phosphate Pathway through SIRT2." Front Biosci (Landmark Ed) **29**(1): 27.

*Benjamini, Y. and Y. Hochberg (1995). "Controlling the False Discovery Rate: A Practical and Powerful Approach to Multiple Testing." Journal of the Royal Statistical Society: Series B (Methodological) **57**(1): 289-300.

*Boleij, A., P. Fathi, W. Dalton, B. Park, X. Wu, D. Huso, J. Allen, S. Besharati, R. A. Anders, F. Housseau, A. E. Mackenzie, L. Jenkins, G. Milligan, S. Wu and C. L. Sears (2021). "G-protein coupled receptor 35 (GPR35) regulates the colonic epithelial cell response to enterotoxigenic Bacteroides fragilis." Commun Biol **4**(1): 585.

*Brennecke, J., A. Stark, R. B. Russell and S. M. Cohen (2005). "Principles of microRNA-target recognition." PLoS Biol **3**(3): e85.

*Chen, Y. and X. Wang (2020). "miRDB: an online database for prediction of functional microRNA targets." Nucleic Acids Res **48**(D1): D127-D131.

*Chong, Z. X., S. K. Yeap and W. Y. Ho (2021). "Unraveling the roles of miRNAs in regulating epithelial-to-mesenchymal transition (EMT) in osteosarcoma." Pharmacol Res **172**: 105818.

*Conceicao-Silva, F. and F. N. Morgado (2019). "Leishmania Spp-Host Interaction: There Is Always an Onset, but Is There an End?" Front Cell Infect Microbiol **9**: 330.

*Cui, C., B. hi, J. Shi, Y. Zhou, VCui and Q. (2019). "Defining the Importance Score of Human MicroRNAs and Their Single Nucleotide Mutants Using Random Forest Regression and Sequence Data." Adv. Theory Simul. **2**(9).

*de La Llave, E., H. Lecoeur, A. Besse, G. Milon, E. Prina and T. Lang (2011). "A combined luciferase imaging and reverse transcription polymerase chain reaction assay for the study of Leishmania amastigote burden and correlated mouse tissue transcript fluctuations." Cell Microbiol **13**(1): 81-91.

*Denzler, R., S. E. McGeary, A. C. Title, V. Agarwal, D. P. Bartel and M. Stoffel (2016). "Impact of MicroRNA Levels, Target-Site Complementarity, and Cooperativity on Competing Endogenous RNA-Regulated Gene Expression." Mol Cell **64**(3): 565-579.

*Dobin, A., C. A. Davis, F. Schlesinger, J. Drenkow, C. Zaleski, S. Jha, P. Batut, M. Chaisson and T. R. Gingeras (2013). "STAR: ultrafast universal RNA-seq aligner." Bioinformatics **29**(1): 15-21.

600 *Fernandes, J. C. R., A. N. A. Goncalves, L. M. Floeter-Winter, H. I. Nakaya and S. M. Muxel (2022).
601 "Comparative transcriptomic analysis of long noncoding RNAs in Leishmania-infected human
602 macrophages." Front Genet **13**: 1051568.
603 *Ganguly, S., B. Ghoshal, I. Banerji, S. Bhattacharjee, S. Chakraborty, A. Goswami, K. Mukherjee and S. N.
604 Bhattacharyya (2022). "Leishmania survives by exporting miR-146a from infected to resident cells to
605 subjugate inflammation." Life Sci Alliance **5**(6).
606 *Geraci, N. S., J. C. Tan and M. A. McDowell (2015). "Characterization of microRNA expression profiles in
607 Leishmania-infected human phagocytes." Parasite Immunol **37**(1): 43-51.
608 *Griffiths-Jones, S., R. J. Grocock, S. van Dongen, A. Bateman and A. J. Enright (2006). "miRBase:
609 microRNA sequences, targets and gene nomenclature." Nucleic Acids Res **34**(Database issue): D140-144.
610 *Grimson, A., K. K. Farh, W. K. Johnston, P. Garrett-Engele, L. P. Lim and D. P. Bartel (2007). "MicroRNA
611 targeting specificity in mammals: determinants beyond seed pairing." Mol Cell **27**(1): 91-105.
612 *Guo, X., H. Qi, G. Lin, J. Yu, M. Zhang and X. Gao (2023). "ARID3A plays a key regulatory role in palmitic
613 acid-stimulated milk fat synthesis in mouse mammary epithelial cells." Cell Biol Int **47**(6): 1106-1117.
614 *Gutierrez Sanchez, M., S. Zhang, C. Gharsallah, S. Lamotte, H. Varet, R. Legendre, F. Dingli, D. Loew, D.
615 Rotili, S. Valente, A. Mai, P. Loiseau, S. Pomel, M. Jung, H. Lecoeur, E. Prina and G. F. Späth (2023).
616 "Inhibition of the macrophage demethylase LSD1 reverses Leishmania amazonensis-induced
617 transcriptomic changes and causes a decrease in parasite load." BioRxiv
618 **doi.org/10.1101/2023.09.29.560133**
619 *Kamhawi, S. and T. D. Serafim (2020). "Leishmania: A Maestro in Epigenetic Manipulation of
620 Macrophage Inflammasomes." Trends Parasitol **36**(6): 498-501.
621 *Kao, T. W., H. H. Chen, J. Lin, T. L. Wang and Y. A. Shen (2024). "PBX1 as a novel master regulator in
622 cancer: Its regulation, molecular biology, and therapeutic applications." Biochim Biophys Acta Rev Cancer
623 **1879**(2): 189085.
624 *Kozomara, A., M. Birgaoanu and S. Griffiths-Jones (2019). "miRBase: from microRNA sequences to
625 function." Nucleic Acids Res **47**(D1): D155-D162.
626 *Krek, A., D. Grun, M. N. Poy, R. Wolf, L. Rosenberg, E. J. Epstein, P. MacMenamin, I. da Piedade, K. C.
627 Gunsalus, M. Stoffel and N. Rajewsky (2005). "Combinatorial microRNA target predictions." Nat Genet
628 **37**(5): 495-500.
629 *Kruger, J. and M. Rehmsmeier (2006). "RNAhybrid: microRNA target prediction easy, fast and flexible."
630 Nucleic Acids Res **34**: W451-454.
631 *Lambert, S. A., A. Jolma, L. F. Campitelli, P. K. Das, Y. Yin, M. Albu, X. Chen, J. Taipale, T. R. Hughes and
632 M. T. Weirauch (2018). "The Human Transcription Factors." Cell **172**(4): 650-665.
633 *Langmead, B., C. Trapnell, M. Pop and S. L. Salzberg (2009). "Ultrafast and memory-efficient alignment
634 of short DNA sequences to the human genome." Genome Biol **10**(3): R25.
635 *Lecoeur, H., E. Prina, M. Gutierrez-Sanchez and G. F. Spath (2022). "Going ballistic: Leishmania nuclear
636 subversion of host cell plasticity." Trends Parasitol **38**(3): 205-216.
637 *Lecoeur, H., E. Prina, T. Rosazza, K. Kokou, P. N'Diaye, N. Aulner, H. Varet, G. Bussotti, Y. Xing, G. Milon,
638 R. Weil, G. Meng and G. F. Spath (2020). "Targeting Macrophage Histone H3 Modification as a
639 Leishmania Strategy to Dampen the NF-kappaB/NLRP3-Mediated Inflammatory Response." Cell Rep
640 **30**(6): 1870-1882 e1874.
641 *Lecoeur, H., T. Rosazza, K. Kokou, H. Varet, J. Y. Coppee, A. Lari, P. H. Commere, R. Weil, G. Meng, G.
642 Milon, G. F. Spath and E. Prina (2020). "Leishmania amazonensis Subverts the Transcription Factor
643 Landscape in Dendritic Cells to Avoid Inflammasome Activation and Stall Maturation." Front Immunol **11**:
644 1098.
645 *Lecoeur, H., S. Zhang, H. Varet, R. Legendre, C. Proux, C. Granjean, P. Bousso, E. Prina and G. F. Späth
646 (2022). "*Leishmania amazonensis* controls macrophage-regulated cell death to establish chronic
647 infection *in vitro* and *in vivo*." bioRxiv: 2022.2009.2014.507851.

648 *Lemaire, J., G. Mkannez, F. Z. Guerfali, C. Gustin, H. Attia, R. M. Sghaier, C. Sysco, K. Dellagi, D. Laouini
649 and P. Renard (2013). "MicroRNA expression profile in human macrophages in response to Leishmania
650 major infection." PLoS Negl Trop Dis **7**(10): e2478.
651 *Lewis, B. P., C. B. Burge and D. P. Bartel (2005). "Conserved seed pairing, often flanked by adenosines,
652 indicates that thousands of human genes are microRNA targets." Cell **120**(1): 15-20.
653 *Lewis, B. P., I. H. Shih, M. W. Jones-Rhoades, D. P. Bartel and C. B. Burge (2003). "Prediction of
654 mammalian microRNA targets." Cell **115**(7): 787-798.
655 *Liao, Y., G. K. Smyth and W. Shi (2014). "featureCounts: an efficient general purpose program for
656 assigning sequence reads to genomic features." Bioinformatics **30**(7): 923-930.
657 *Litvak-Greenfeld, D. and I. Benhar (2012). "Risks and untoward toxicities of antibody-based
658 immunoconjugates." Adv Drug Deliv Rev **64**(15): 1782-1799.
659 *Liu, Q., M. K. Novak, R. M. Pepin, T. Eich and W. Hu (2021). "microRNA-mediated regulation of
660 microRNA machinery controls cell fate decisions." Elife **10**.
661 *Lorenz, R., S. H. Bernhart, C. Honer Zu Siederdissen, H. Tafer, C. Flamm, P. F. Stadler and I. L. Hofacker
662 (2011). "ViennaRNA Package 2.0." Algorithms Mol Biol **6**: 26.
663 *Love, M. I., W. Huber and S. Anders (2014). "Moderated estimation of fold change and dispersion for
664 RNA-seq data with DESeq2." Genome Biol **15**(12): 550.
665 *Luna, J. M., T. K. Scheel, T. Danino, K. S. Shaw, A. Mele, J. J. Fak, E. Nishiuchi, C. N. Takacs, M. T.
666 Catanese, Y. P. de Jong, I. M. Jacobson, C. M. Rice and R. B. Darnell (2015). "Hepatitis C virus RNA
667 functionally sequesters miR-122." Cell **160**(6): 1099-1110.
668 *Marr, A. K., J. L. MacIsaac, R. Jiang, A. M. Airo, M. S. Kobor and W. R. McMaster (2014). "Leishmania
669 donovani infection causes distinct epigenetic DNA methylation changes in host macrophages." PLoS
670 Pathog **10**(10): e1004419.
671 *Martinez-Hernandez, J. E., Z. Hammoud, A. M. de Sousa, F. Kramer, R. L. D. Monte-Neto, V. Maracaja-
672 Coutinho and A. J. M. Martin (2021). "Network-Based Approaches Reveal Potential Therapeutic Targets
673 for Host-Directed Antileishmanial Therapy Driving Drug Repurposing." Microbiol Spectr **9**(2): e0101821.
674 *McGeary, S. E., K. S. Lin, C. Y. Shi, T. M. Pham, N. Bisaria, G. M. Kelley and D. P. Bartel (2019). "The
675 biochemical basis of microRNA targeting efficacy." Science **366**(6472).
676 *McGwire, B. S. and A. R. Satoskar (2014). "Leishmaniasis: clinical syndromes and treatment." QJM
677 **107**(1): 7-14.
678 *Mishra, R., S. Mohanty, S. Mahapatra and P. Prasad (2023). "Overview of microbial therapeutics in
679 immunological disorders." Microbiome Therapeutics: 289-353.
680 *Mukherjee, B., J. Paul, S. Mukherjee, R. Mukhopadhyay, S. Das, K. Naskar, S. Sundar, J. C. Dujardin, B.
681 Saha and S. Roy (2015). "Antimony-Resistant Leishmania donovani Exploits miR-466i To Deactivate Host
682 MyD88 for Regulating IL-10/IL-12 Levels during Early Hours of Infection." J Immunol **195**(6): 2731-2742.
683 *Murdaca, G., A. Tonacci, S. Negrini, M. Greco, M. Borro, F. Puppo and S. Gangemi (2019). "Effects of
684 AntagomiRs on Different Lung Diseases in Human, Cellular, and Animal Models." Int J Mol Sci **20**(16).
685 *Muxel, S. M., S. M. Acuna, J. I. Aoki, R. A. Zampieri and L. M. Floeter-Winter (2018). "Toll-Like Receptor
686 and miRNA-let-7e Expression Alter the Inflammatory Response in Leishmania amazonensis-Infected
687 Macrophages." Front Immunol **9**: 2792.
688 *Muxel, S. M., M. F. Laranjeira-Silva, R. A. Zampieri and L. M. Floeter-Winter (2017). "Leishmania
689 (Leishmania) amazonensis induces macrophage miR-294 and miR-721 expression and modulates
690 infection by targeting NOS2 and L-arginine metabolism." Sci Rep **7**: 44141.
691 *Nandan, D., C. T. Rath and N. E. Reiner (2021). "Leishmania regulates host macrophage miRNAs
692 expression by engaging transcription factor c-Myc." J Leukoc Biol **109**(5): 999-1007.
693 *Osorio y Fortea, J., E. de La Llave, B. Regnault, J. Y. Coppee, G. Milon, T. Lang and E. Prina (2009).
694 "Transcriptional signatures of BALB/c mouse macrophages housing multiplying Leishmania amazonensis
695 amastigotes." BMC Genomics **10**: 119.

696 *Pasquinelli, A. E., B. J. Reinhart, F. Slack, M. Q. Martindale, M. I. Kuroda, B. Maller, D. C. Hayward, E. E.
697 Ball, B. Degnan, P. Muller, J. Spring, A. Srinivasan, M. Fishman, J. Finnerty, J. Corbo, M. Levine, P. Leahy,
698 E. Davidson and G. Ruvkun (2000). "Conservation of the sequence and temporal expression of let-7
699 heterochronic regulatory RNA." Nature **408**(6808): 86-89.
700 *Patterson, E. S., R. C. Addis, M. J. Shamblott and J. D. Gearhart (2008). "SOX17 directly activates Zfp202
701 transcription during in vitro endoderm differentiation." Physiol Genomics **34**(3): 277-284.
702 *Pikuleva, I. A., A. Babiker, M. R. Waterman and I. Bjorkhem (1998). "Activities of recombinant human
703 cytochrome P450c27 (CYP27) which produce intermediates of alternative bile acid biosynthetic
704 pathways." J Biol Chem **273**(29): 18153-18160.
705 *Popenda, M., M. Szachniuk, M. Antczak, K. J. Purzycka, P. Lukasiak, N. Bartol, J. Blazewicz and R. W.
706 Adamiak (2012). "Automated 3D structure composition for large RNAs." Nucleic Acids Res **40**(14): e112.
707 *Quazi, F. and R. S. Molday (2013). "Differential phospholipid substrates and directional transport by
708 ATP-binding cassette proteins ABCA1, ABCA7, and ABCA4 and disease-causing mutants." J Biol Chem
709 **288**(48): 34414-34426.
710 *R-Core-Team (2016). "R: A Language and Environment for Statistical Computing. R Foundation for
711 Statistical Computing." https://www.R-project.org/.
712 *Ramos-Sanchez, E. M., L. C. Reis, M. A. Souza, S. M. Muxel, K. R. Santos, D. Lagos, V. R. A. Pereira, M. E.
713 F. de Brito, P. M. Kaye, L. M. Floeter-Winter and H. Goto (2022). "miR-548d-3p Is Up-Regulated in Human
714 Visceral Leishmaniasis and Suppresses Parasite Growth in Macrophages." Front Cell Infect Microbiol **12**:
715 826039.
716 *Rashidi, S., R. Mansouri, M. Ali-Hassanzadeh, E. Ghani, A. Barazesh, M. Karimazar, P. Nguewa and E. A.
717 Carrera Silva (2021). "Highlighting the interplay of microRNAs from Leishmania parasites and infected-
718 host cells." Parasitology **148**(12): 1434-1446.
719 *Riolo, G., S. Cantara, C. Marzocchi and C. Ricci (2020). "miRNA Targets: From Prediction Tools to
720 Experimental Validation." Methods Protoc **4**(1).
721 *Rupaimoole, R. and F. J. Slack (2017). "MicroRNA therapeutics: towards a new era for the management
722 of cancer and other diseases." Nat Rev Drug Discov **16**(3): 203-222.
723 *Shalgi, R., D. Lieber, M. Oren and Y. Pilpel (2007). "Global and local architecture of the mammalian
724 microRNA-transcription factor regulatory network." PLoS Comput Biol **3**(7): e131.
725 *Shannon, P., A. Markiel, O. Ozier, N. S. Baliga, J. T. Wang, D. Ramage, N. Amin, B. Schwikowski and T.
726 Ideker (2003). "Cytoscape: a software environment for integrated models of biomolecular interaction
727 networks." Genome Res **13**(11): 2498-2504.
728 *Smith, T., A. Heger and I. Sudbery (2017). "UMI-tools: modeling sequencing errors in Unique Molecular
729 Identifiers to improve quantification accuracy." Genome Res **27**(3): 491-499.
730 *Spath, G. F., P. Schlesinger, R. Schreiber and S. M. Beverley (2009). "A novel role for Stat1 in phagosome
731 acidification and natural host resistance to intracellular infection by Leishmania major." PLoS Pathog
732 **5**(4): e1000381.
733 *Sprenkle, N. T., C. H. Serezani and H. H. Pua (2023). "MicroRNAs in Macrophages: Regulators of
734 Activation and Function." J Immunol **210**(4): 359-368.
735 *Sun, X., S. Hua, H. R. Chen, Z. Ouyang, K. Einkauf, S. Tse, K. Ard, A. Ciaranello, S. Yawetz, P. Sax, E. S.
736 Rosenberg, M. Lichterfeld and X. G. Yu (2017). "Transcriptional Changes during Naturally Acquired Zika
737 Virus Infection Render Dendritic Cells Highly Conducive to Viral Replication." Cell Rep **21**(12): 3471-3482.
738 *Supek, F., M. Bosnjak, N. Skunca and T. Smuc (2011). "REVIGO summarizes and visualizes long lists of
739 gene ontology terms." PLoS One **6**(7): e21800.
740 *Taghehchian, N., Y. Samsami, A. Maharati, A. S. Zangouei, S. Boroumand-Noughabi and M. Moghbeli
741 (2023). "Molecular biology of microRNA-342 during tumor progression and invasion." Pathol Res Pract
742 **248**: 154672.

743 *Tai, M. C., T. Kajino, M. Nakatochi, C. Arima, Y. Shimada, M. Suzuki, H. Miyoshi, Y. Yatabe, K. Yanagisawa
744 and T. Takahashi (2015). "miR-342-3p regulates MYC transcriptional activity via direct repression of E2F1
745 in human lung cancer." Carcinogenesis **36**(12): 1464-1473.
746 *Thammaiah, C. K. and S. Jayaram (2016). "Role of let-7 family microRNA in breast cancer." Noncoding
747 RNA Res **1**(1): 77-82.
748 *Tiwari, N., V. Kumar, M. R. Gedda, A. K. Singh, V. K. Singh, S. Gannavaram, S. P. Singh and R. K. Singh
749 (2017). "Identification and Characterization of miRNAs in Response to Leishmania donovani Infection:
750 Delineation of Their Roles in Macrophage Dysfunction." Front Microbiol **8**: 314.
751 *Trimarchi, J. M., B. Fairchild, J. Wen and J. A. Lees (2001). "The E2F6 transcription factor is a component
752 of the mammalian Bmi1-containing polycomb complex." Proc Natl Acad Sci U S A **98**(4): 1519-1524.
753 *Tsang, J., J. Zhu and A. van Oudenaarden (2007). "MicroRNA-mediated feedback and feedforward loops
754 are recurrent network motifs in mammals." Mol Cell **26**(5): 753-767.
755 *Valinezhad Orang, A., R. Safaralizadeh and M. Kazemzadeh-Bavili (2014). "Mechanisms of miRNA-
756 Mediated Gene Regulation from Common Downregulation to mRNA-Specific Upregulation." Int J
757 Genomics **2014**: 970607.
758 *Wang, T., T. Zhou, F. Fu, Y. Han, Y. Li and M. Yuan (2022). "HMGA1 As a Potential Prognostic and
759 Therapeutic Biomarker in Breast Cancer." Dis Markers **2022**: 7466555.
760 *Xu, L., Z. Wang and G. Wang (2024). "Screening of Biomarkers Associated with Osteoarthritis Aging
761 Genes and Immune Correlation Studies." Int J Gen Med **17**: 205-224.
762 *Zhang, L., H. Guo, X. Zhang, L. Wang, F. Wei, Y. Zhao, B. Wang, Y. Meng and Y. Li (2024). "Small nucleolar
763 RNA Snora73 promotes psoriasis progression by sponging miR-3074-5p and regulating PBX1 expression."
764 Funct Integr Genomics **24**(1): 15.
765 *Zhang, P., W. Wu, Q. Chen and M. Chen (2019). "Non-Coding RNAs and their Integrated Networks." J
766 Integr Bioinform **16**(3).
767 *Zhang, S., H. Lecoeur, H. Varet, R. Legendre, N. Mahtal, C. Proux, N. Aulner, S. Shorte, C. Granjean, P.
768 Bousso, E. Prina and G. F. Späth (2022). "Immunometabolic profiling of in vitro and ex vivo *Leishmania*-
769 infected macrophages (LIMs) reveals unique polarization and bioenergetic signatures." BioRxiv:
770 2022.2009.2008.507100.

771

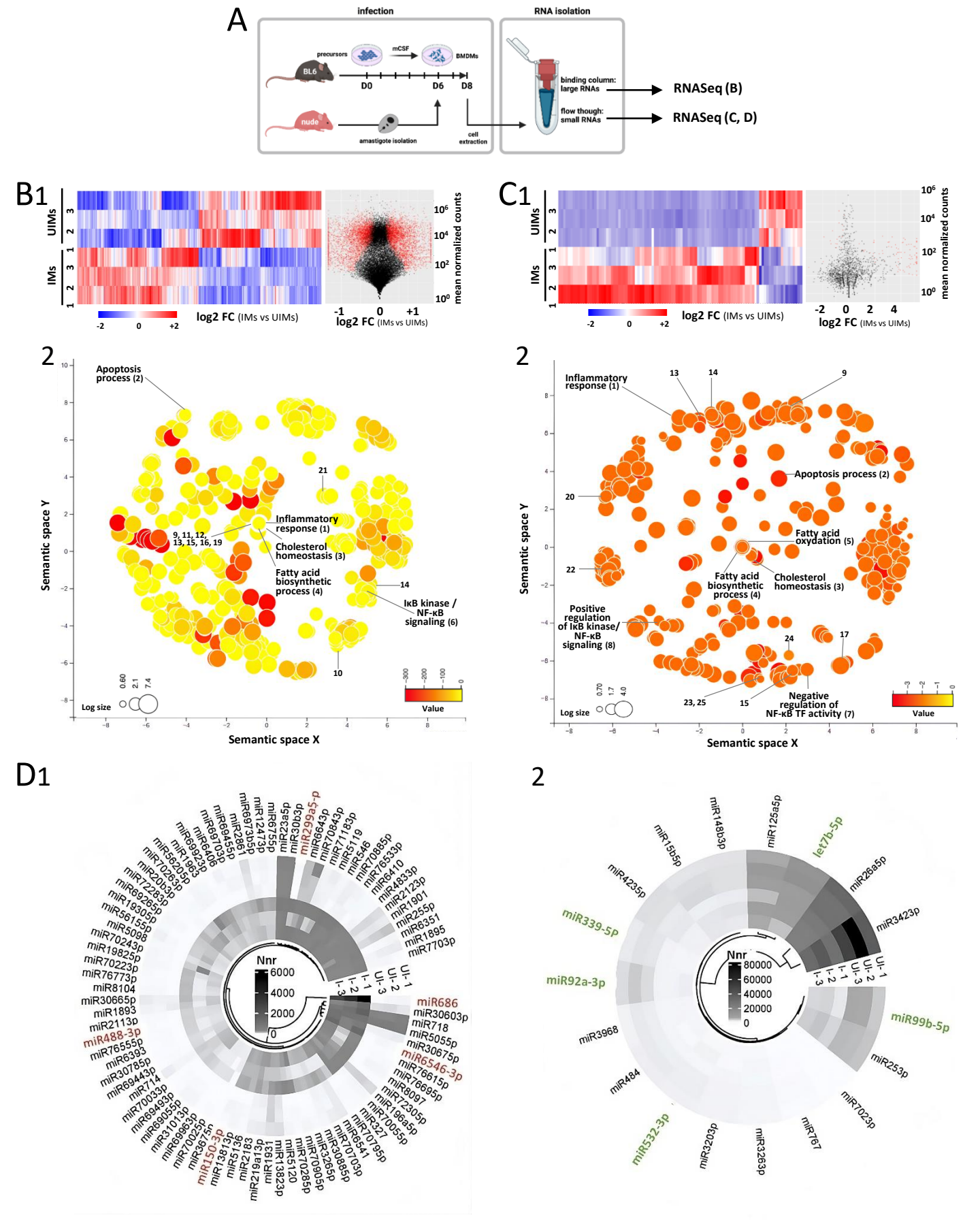

FIGURE 1, Gharsallah et al.

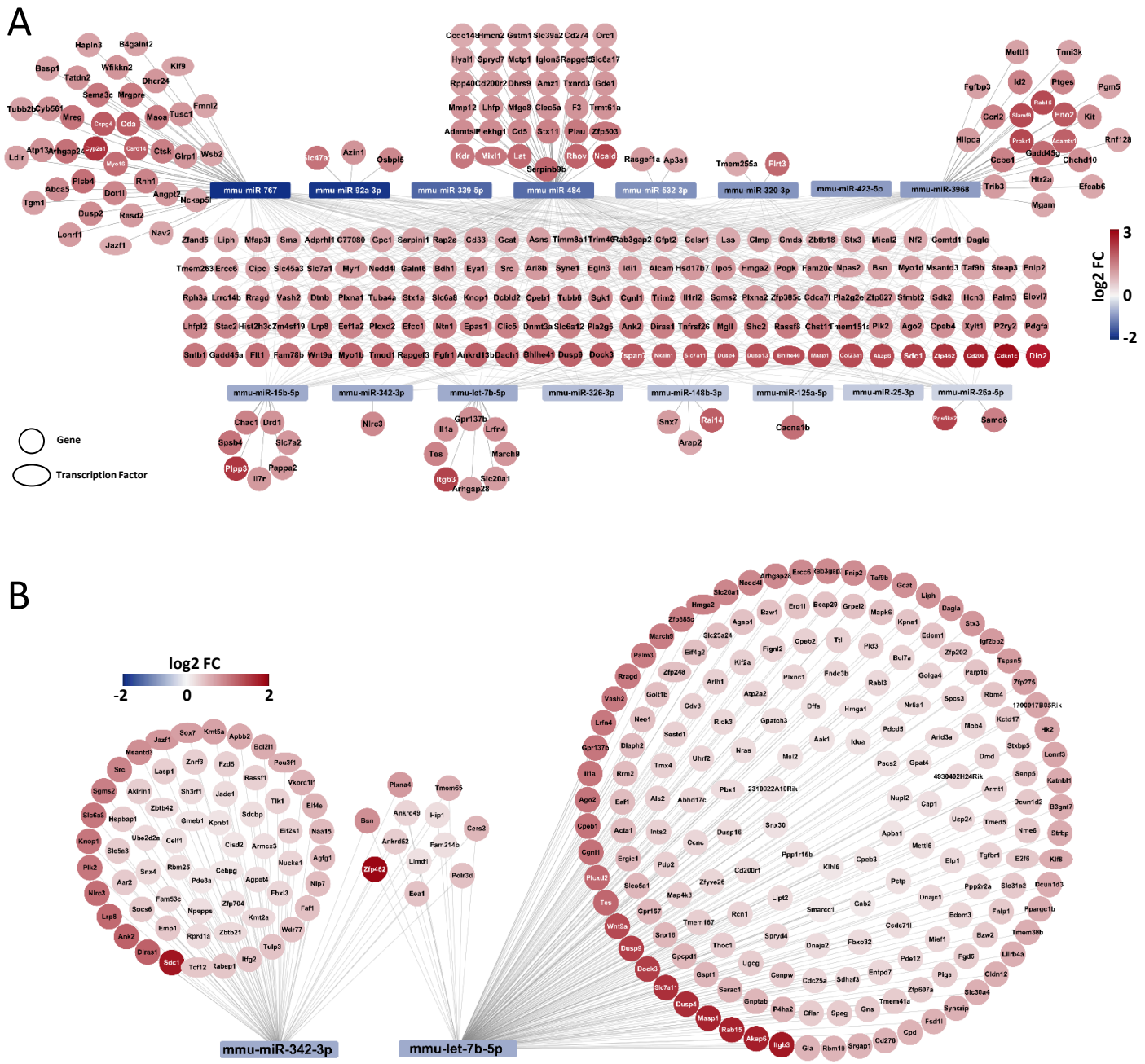

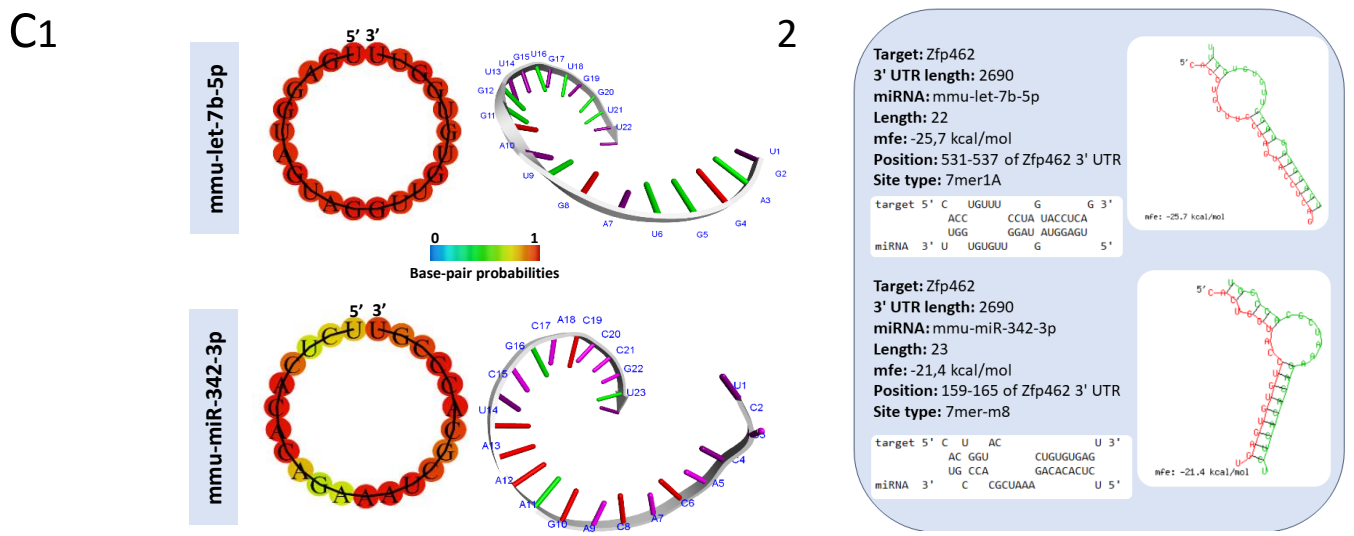

FIGURE 2, Gharsallah et al.

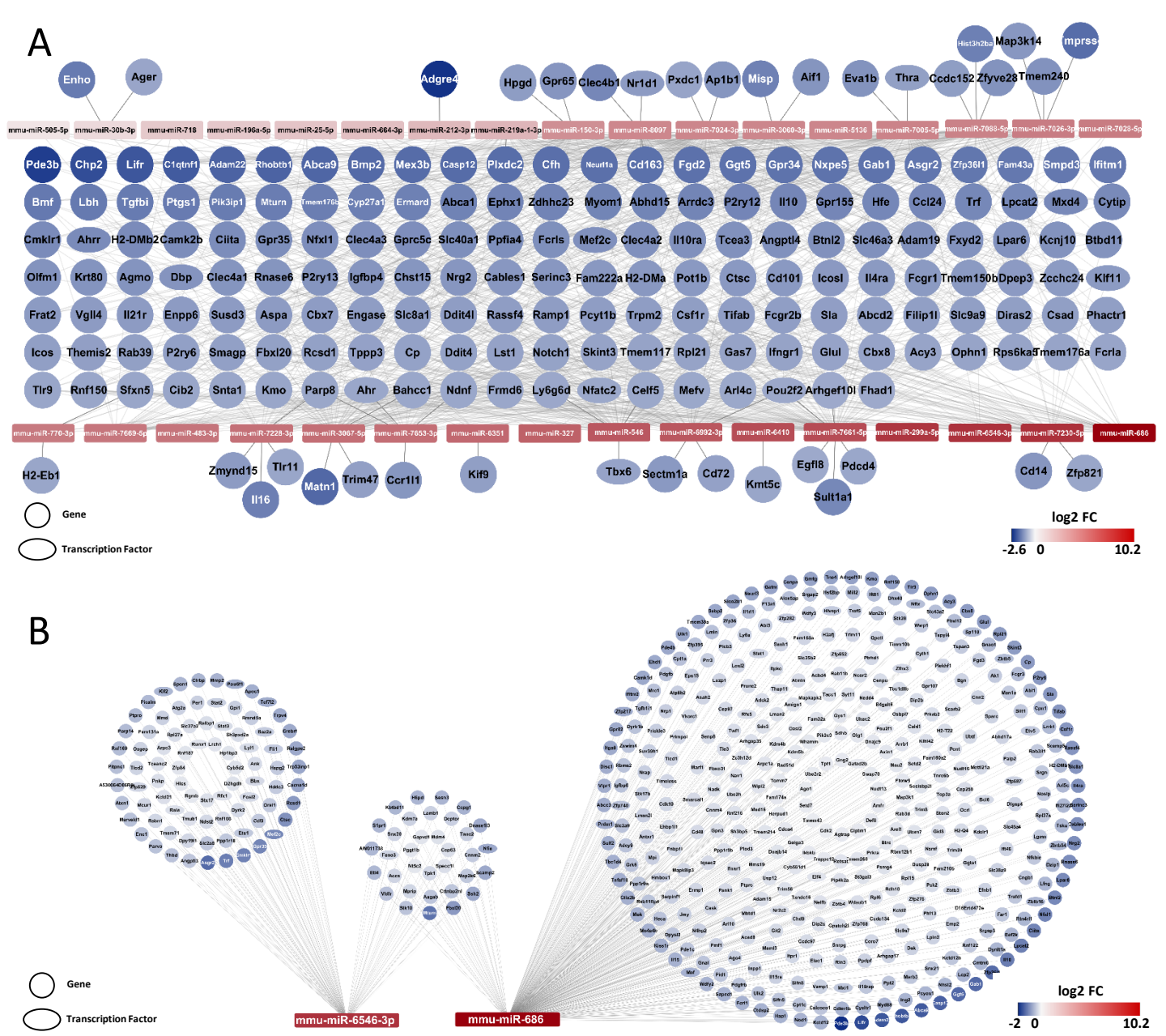

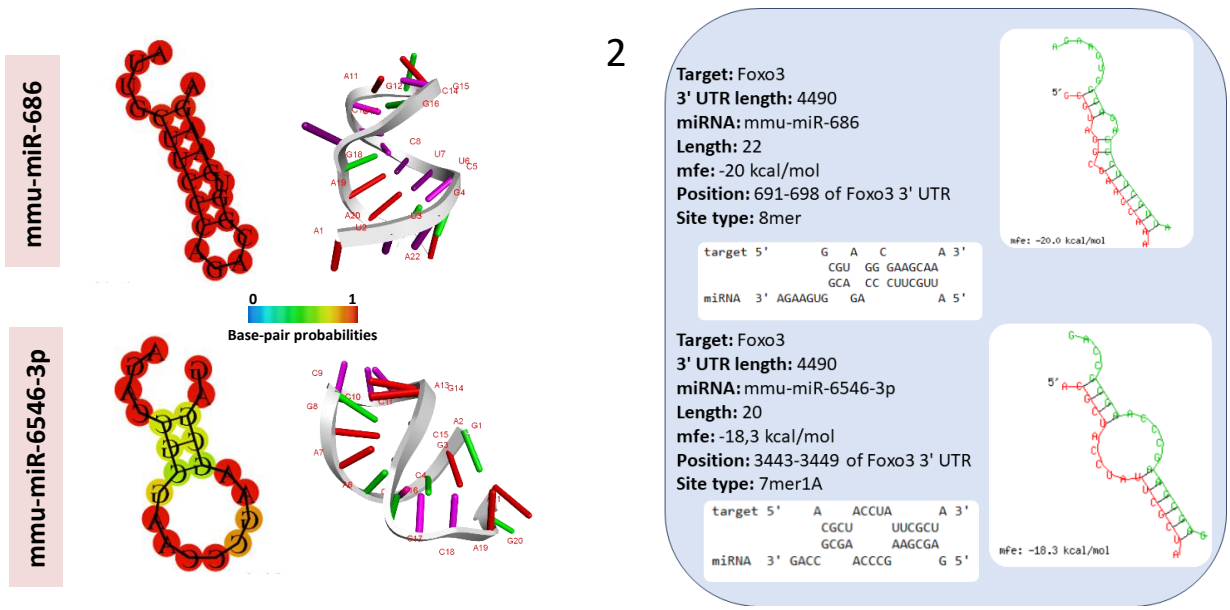

FIGURE 3, Gharsallah et al.

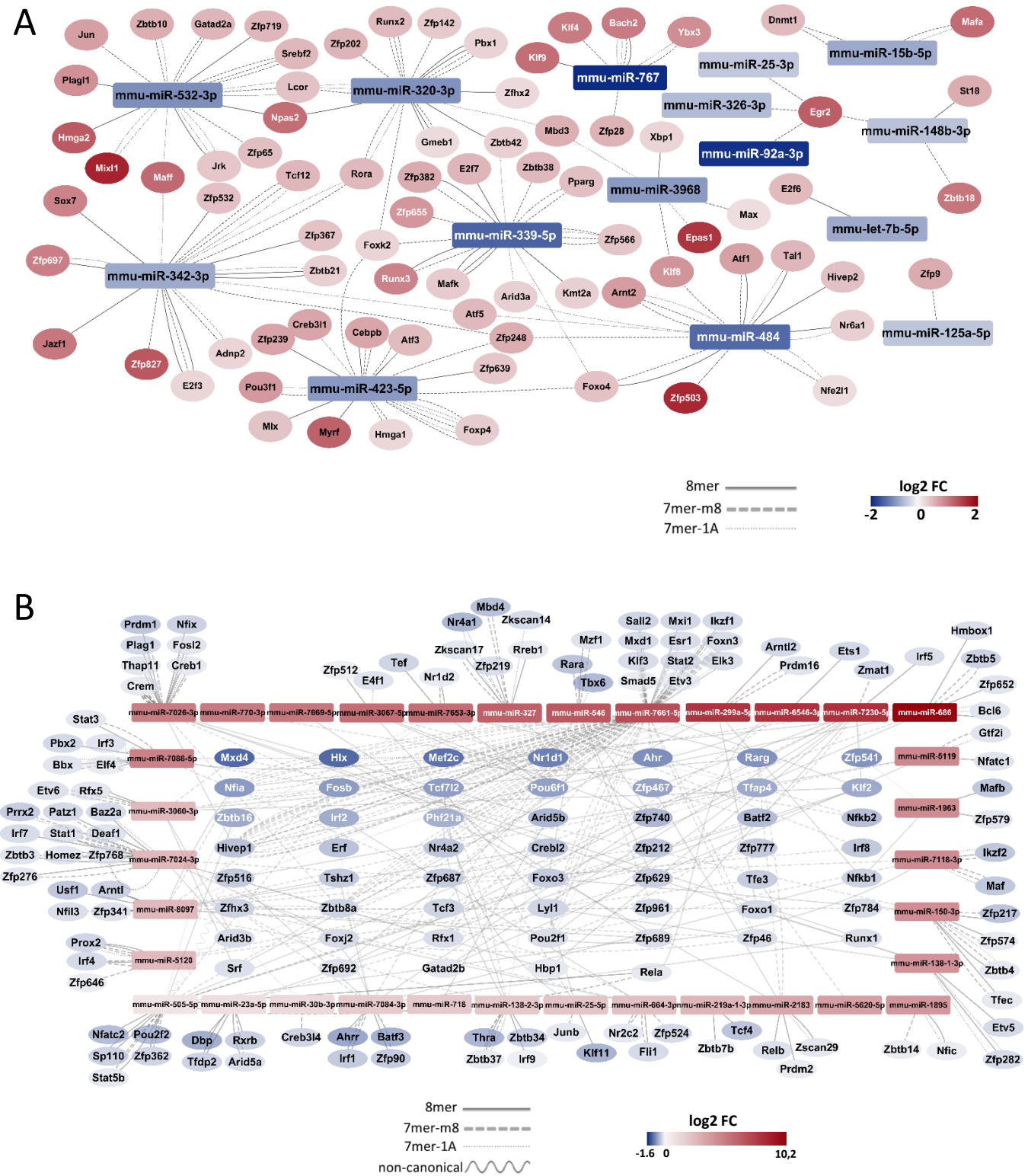

FIGURE 4, Gharsallah et al.

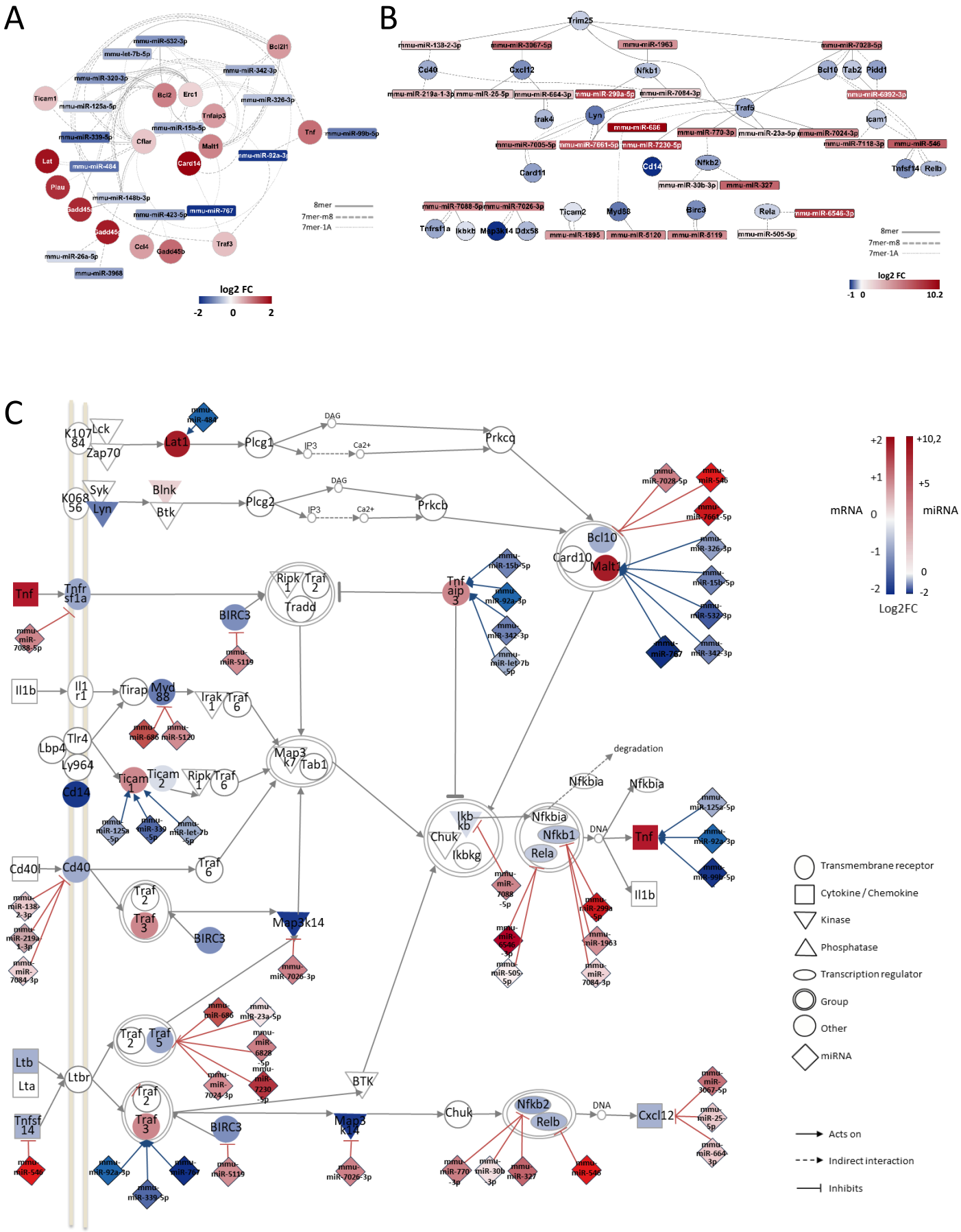

FIGURE 5, Gharsallah et al.

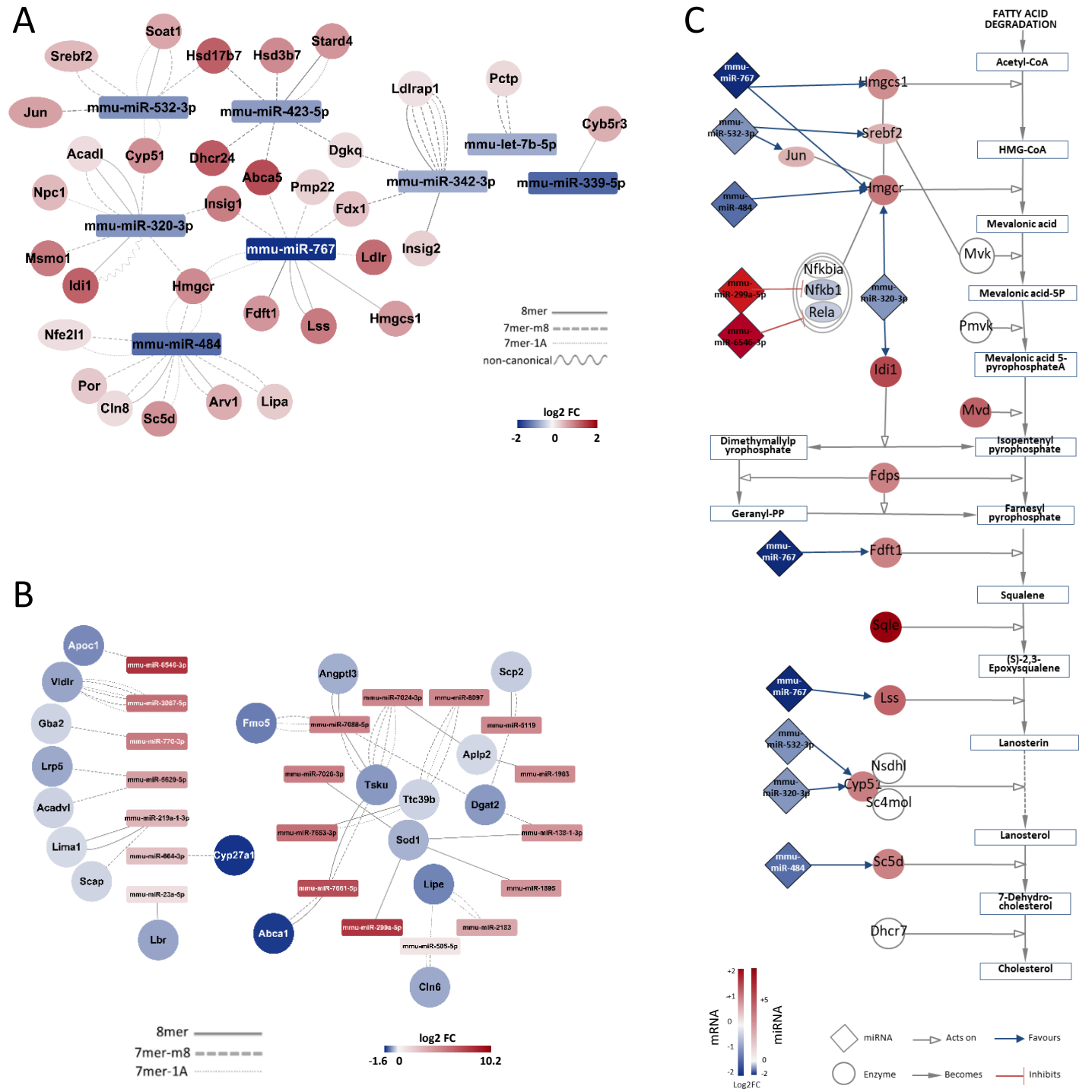

FIGURE 6, Gharsallah et al.